PHOTOSYNTHETICA
International Journal for Photosynthesis Research

DOI 10.32615/ps.2022.012 PHOTOSYNTHETICA 60 (2): 240-250, 2022

Leaf structure and photosynthesis in *Populus alba* under naturally fluctuating environments

X.Y. LIN[*,**,***], X.X. WANG[***], Q.Y. ZENG[*,**,***], and Q. YANG[***,#,+]

State Key Laboratory of Systematic and Evolutionary Botany, Institute of Botany, Chinese Academy of Sciences, 100093 Beijing, China[*]
University of Chinese Academy of Sciences, 100049 Beijing, China[**]
State Key Laboratory of Tree Genetics and Breeding, Chinese Academy of Forestry, 100091 Beijing, China[***]
State Key Laboratory of Subtropical Silviculture, College of Forestry and Biotechnology, Zhejiang A&F University, Hangzhou, 311300 Zhejiang, China[#]

Abstract

The ability to modulate photosynthesis is essential for plants to adapt to fluctuating growing conditions. *Populus* species show high tolerance to various and highly variable environments. To understand their response strategies against fluctuating environments, this study investigated the morphological and physiological differences of white poplar (*Populus alba*) leaves when grown in a phytotron, glasshouse, and field. Our results show that the palisade cells were elongated in the field, which would enhance intercellular CO_2 exchange. Photosynthetic capacity was the highest in the field leaves, as shown by higher electron transport rates (1.8 to 6.5 times) and carbon assimilation rates (2.7 to 4.2 times). The decrease of PSI acceptor-side limitation and increase of PSI donor-side limitation suggests changes in PSI redox status may contribute to photoprotection. This plasticity of white poplar allows adjusting its structure and photosynthesis under fluctuating conditions, which may partly enable its outstanding tolerance against environmental changes.

Keywords: fluctuating conditions; photoinhibition; photosynthesis; plasticity; *Populus alba*.

Highlights

- The leaf structure is modified to enhance intercellular CO_2 exchange in the field
- Rubisco ability is functionally balanced with electron transfer
- The regulation of NPQ and PSI redox status contributes to photoprotection

Received 18 October 2021
Accepted 23 February 2022
Published online 28 March 2022

[+]Corresponding author
e-mail: qiyang@zafu.edu.cn

Abbreviations: A_c – the limitation by RuBP carboxylation; A_j – the limitation by RuBP regeneration; Chl – chlorophyll; C_i – intercellular CO_2 concentration; DEPS – de-epoxidation states of the xanthophyll cycle; DMA – leaf dry mass per area; $ETR_{(I)}$ – electron transport rate of PSI; $ETR_{(II)}$ – electron transport rate of PSII; F_v/F_m – maximum photochemical efficiency of PSII; g_m – mesophyll conductance; g_s – stomatal conductance; J_{max} – maximum electron transport rate; LMA – leaf mass per area; M_A – leaf dry mass per unit area; MDA – malondialdehyde content; MF – grown under field conditions with leaf samples about four months old; MG – grown in the glasshouse with leaf samples about four months old; NPQ – nonphotochemical quenching; NSC – nonstructural carbohydrates; P_N – saturating CO_2 assimilation rate at 400 ppm CO_2 concentration; R_d – respiration rate in light; S_{mes}/S – mesophyll surface area exposed to intercellular air space per leaf area; TEM – transmission electron micrographs; t_{leaf} – leaf thickness; VAZ – total xanthophyll cycle pigments; V_{cmax} – maximum carboxylation rate; WUE – water-use efficiency; $Y_{(I)}$ – actual photochemical efficiency of PSI; $Y_{(II)}$ – actual photochemical efficiency of PSII; YC – grown in the phytotron with leaf samples about four months old; YG – grown in the glasshouse with leaf samples about two months old; $Y_{(NA)}$ – acceptor-side limitation of PSI; $Y_{(ND)}$ – donor-side limitation of P_{700}.

Acknowledgments: The authors acknowledge the technical assistance of Dr. Yuan Cao for the electron microscopy photographing. The authors would like to express gratitude to *EditSprings* (https://www.editsprings.cn/) for the expert linguistic services provided. We thank two anonymous reviewers for their constructive comments. This work was supported by the Fundamental Research Funds of Chinese Academy of Forestry (CAFYBB2018ZX001) and the Scientific Development and Research Foundation of Zhejiang A&F University (203402017601).

Conflict of interest: The authors declare that they have no conflict of interest.

Introduction

Plants are constantly exposed to transient, diurnal, and seasonal changes of various environmental factors (Demmig-Adams *et al.* 2012). Light, temperature, and water availability influence plant physiological performance and can eventually affect their fitness (Korotaeva *et al.* 2015, Allakhverdiev 2020). During the last few decades, climate change has caused more severe and frequent drought and heat stresses due to anthropogenic forces and will continue to do so (IPCC 2014). These more extreme conditions will be challenging for forests to adapt to (Stefanski *et al.* 2020). The ability of tree species to accommodate such changes in environmental conditions presumes phenotypic and physiological plasticity.

The adaptation of trees to new growing conditions largely relies on photosynthesis (Li *et al.* 2009). Light has a fundamental role in tree growth and development and varies remarkably under natural conditions (Kono *et al.* 2017). The photon flux reaching vegetation varies constantly during the day and across seasons mainly due to changes in sun and clouds and the wind-induced movement of the canopy (Allahverdiyeva *et al.* 2015). With increasing light intensity, light absorption may exceed photosynthetic utilization. This mismatch between excitation of photosynthetic pigments and the ability to use the excitation energy will generate reactive molecules such as reactive oxygen species (ROS) that oxidize lipids and proteins in chloroplasts, resulting in photoinhibition (Ahmad *et al.* 2010, 2019; Demmig-Adams and Adams 2018, Kohli *et al.* 2019). The morphological, anatomical, and physiological traits of leaves thus display sensitivity and plasticity to light conditions to ensure a proper balance of light absorption and usage (Way and Pearcy 2012, Huang *et al.* 2021). For example, compared to shaded leaves, leaves under high light have a higher leaf mass per area (LMA), total dry mass, thickness, and stomatal density, and also more chloroplasts per unit of exposed mesophyll surface area (Tosens *et al.* 2012, Dlugos *et al.* 2015, Zadworny *et al.* 2018).

The supply of light usually fluctuates independently of other environmental factors that affect photosynthetic utilization (Brestic *et al.* 2021). Consequent combinations such as bright sunlight and water or heat stresses also cause photoinhibition in leaf cells. Plants have thus evolved several adaptation mechanisms of photosynthesis regulation that are crucial for photoprotection under fluctuating light and/or environmental stress conditions (Schumann *et al.* 2017). At the stage of excitation energy transfer in the antenna beds, excess energy can be efficiently dissipated or leaked as heat *via* carotenoid- and chlorophyll-related pathways (Ware *et al.* 2015, Li *et al.* 2018). At the stage of electron transport systems, electrons can be efficiently leaked *via* cyclic electron flow around the reaction centers due to changes in redox potential or the stability of the reactants (Shikanai and Yamamoto 2017). The water–water cycle and photorespiration are also effective protective mechanisms. At the thylakoid membrane level, the rate of D1 protein turnover as proposed by the damage repair cycle and photosynthetic protein complexes can be regulated and reorganized (Kirchhoff 2014, Demmig-Adams *et al.* 2015).

Highly dynamic light and water availability are the key stresses in temperate forests, so it is pertinent to understand the plasticity and mechanisms of morphological, anatomical, and photosynthetic responses to these factors in temperate trees. The degree and nature of photosynthetic acclimation are highly variable between species, even within the same genus. There is still much uncertainty regarding the photosynthesis regulation strategies and acclimation responses of trees (Saxe *et al.* 2002).

Poplars (*Populus* sp.) represent the most widely distributed and cultivated tree species in temperate and boreal regions throughout the Northern Hemisphere (Hozain *et al.* 2010, Müller *et al.* 2012). *Populus* species show high tolerance to various environments and are important subjects in global climate change research (Hozain *et al.* 2010). However, despite *Populus* being a model system for molecular biology and genetic studies of forest trees, we still lack knowledge about their regulatory mechanisms in response to fluctuating environments. The white poplar (*Populus alba* L.), commonly called abele or silver poplar, is a fast-growing species with the capacity to adapt to various stress conditions (Brundu *et al.* 2008, Liu *et al.* 2019). This study aimed to investigate the morphological and physiological regulatory responses of white poplar towards fluctuating environments by comparing fully expanded leaves on plantlets grown under a phytotron, in a sunlit glasshouse, and the field, representing a continuum from stable to highly variable conditions.

Materials and methods

Plant materials and growth conditions: Clonal poplar (*P. alba* L.) plantlets were transplanted from tissue culture bottles to 1-L pots with soil in February 2019 and grown in a phytotron at 25°C and a 16-h photoperiod [PAR of 120 µmol(photon) m^{-2} s^{-1}] for one month. Subsequently, in March, the clonal plantlets were divided into three groups and transplanted to 10-L pots grown in a sunlit glasshouse of the Chinese Academy of Forestry in Beijing under semi-natural conditions with about 90% sunlight and temperature ranging from 24 to 28°C. One group was transplanted in May to an open field in Beijing, China (40°2'N, 115°50'E), and grown under field conditions with full sunlight, 12 to 15-h photoperiod, and average temperature 21 to 28°C (the MF group). Among the remaining plants in the glasshouse, the plantlets from one group were lopped in July to promote sprouting with new shoots (the YG group), while another group was left alone (the MG group). In addition, freshly subcultured clonal poplar was transplanted to soil in July 2019 and grown in the phytotron under conditions as described above (the YC group). Six replicate plants were used in each group. All poplar plants were watered and fertilized regularly. The 3rd and 4th fully expanded leaves, which developed under each growth condition, were used as experimental subjects for anatomical and physiological analysis. By

September 2019, when the samples were collected and measured, the MF and MG leaves were about four months old and the YC and YG leaves were about two months old. The roots were also collected for carbohydrate analysis.

Gas-exchange measurements and calculation of conductance: The measurements were performed from 9:00 to 11:00 h in the morning on sunny days from 25 September to 10 October 2019. The rates of CO_2 assimilation were measured with a *Li-6400* (*Li-Cor*, Lincoln, NE, USA). Net assimilation rates (P_N) were recorded with a CO_2 concentration (C_a) of 400 µmol mol^{-1} at a saturating light intensity of 1,000 µmol(photon) m^{-2} s^{-1}, which is when a steady-state CO_2 exchange is achieved (Ensminger *et al.* 2008). As the YC leaves could not fully cover the measurement chamber, their projected leaf area was measured by *ImageJ* (*version 1.51j8*, National Institute of Health). For the P_N/C_i curves, photosynthesis was measured at 400, 200, 100, 50, 0, 400, 600, 800; 1,000; 1,200; and 1,400 µmol(CO_2) mol^{-1} at a saturating irradiance of 1,000 µmol(photon) m^{-2} s^{-1} as described by Bigras and Bertrand (2006). All measurements were performed at 20°C with 4–6 biological replicates. The maximum carboxylation rate (V_{cmax}), maximum electron transport rate (J_{max}), respiration rate in light (R_d), and mesophyll conductance (g_m) were estimated according to Sharkey *et al*. (2007). The limiting step of photosynthesis was assuming either a Rubisco (A_c) or RuBP regeneration (A_j) limitation, and the A_c and A_j were modeled according to Farquhar *et al*. (1980). The water-use efficiency was calculated as the ratio of P_N to the transpiration rate (WUE = P_N/E). The stomatal limitations were calculated as the ratio of P_N to C_i.

***In vivo* chlorophyll (Chl) fluorescence and P_{700} measurement**: The same leaf was used for Chl fluorescence measurements right after gas-exchange measurements. *In vivo* Chl *a* fluorescence and signals from oxidized P_{700} were monitored simultaneously with a *Dual PAM-F* fluorometer (*Walz*, Effeltrich, Germany) at room temperature. Leaves were dark-acclimated for 30 min. Saturation pulse [10,000 µmol(photon) m^{-2} s^{-1} for 300 ms] was applied with a sequence of increasing actinic light intensity [from 0 to 2,800 µmol(photon) m^{-2} s^{-1}] at the end of each light application. For nonphotochemical quenching (NPQ) determination, the actinic light [1,455 µmol(photon) m^{-2} s^{-1}] was turned on for 5 min and followed by darkness for 5 min with a saturating pulse every 30 seconds. For fluctuating light measurements, the leaves were exposed three times to fluctuating light of 59 µmol(photon) m^{-2} s^{-1} for 5 min and 1,455 µmol(photon) m^{-2} s^{-1} for 1 min. The maximum Chl fluorescence after the dark acclimation (F_m) and during illumination (F_m') was determined. The P_{700} signal (P) was calculated as the difference between the 830 and 875 nm transmittance signals. Photosynthetic parameters were calculated as described in the literature (Baker 2008, Pfündel *et al.* 2008). The F_v/F_m (maximum quantum yield of PSII) and NPQ were calculated as $(F_m - F_0)/F_m$ and $(F_m - F_m')/F_m'$, respectively. The relative $ETR_{(II)}$ (the electron transport rate of PSII) and $ETR_{(I)}$ (the electron transport rate of PSI) were calculated as $Y_{(II)}$ × light intensity [µmol(photon) m^{-2} s^{-1}] and $Y_{(I)}$ × light intensity [µmol(photon) m^{-2} s^{-1}], respectively. $Y_{(ND)}$ (quantum yield of nonphotochemical energy dissipation in PSI reaction centers that are limited due to a shortage of electrons) and $Y_{(NA)}$ (quantum yield of nonphotochemical energy dissipation in PSI reaction centers that are limited due to shortage of electron acceptors) were calculated as $(P - P_0)/P_m$ and $(P_m - P_m')/P_m$, respectively. Data are presented as mean ± SD of six independent measurements.

Light and electron microscopy: After gas-exchange and Chl fluorescence measurements, leaf samples were taken from intercostal areas avoiding big vessels at noon, then prepared with a modified procedure according to Zhang *et al.* (2011). Leaf samples were fixed in 3% glutaraldehyde (v/v) in 0.1 M PBS (sodium phosphate buffer, pH 7.2) for 6–8 h, postfixed in 1% osmium tetraoxide (OsO_4) overnight, and dehydrated with an ethanol series increasing in the concentration by 10% from 30 to 100%, followed by acetone. Then the samples were embedded in *Spurr* epoxy medium. Ultra-thin sections and semi-thin sections were cut using a *Leica EM UC7* ultramicrotome (Germany), then mounted on copper grids and stained with 5% uranyl acetate (dissolved in MQ water) and Reynolds lead citrate. Whole cells and chloroplasts were photographed with an *HT7700* transmission electron microscope (*HITACHI*, Tokyo, Japan). Semi-thin sections for light microscopy were stained with toluidine blue and viewed in the bright field with an *OLYMPUS-BX51* optical microscope (Japan) and photographed with an *Olympus DP74* digital camera (Japan).

Leaf structural analysis: The whole leaf thickness and the palisade and spongy mesophyll ratios were measured from images of light microscopy. Mesophyll surface area exposed to intercellular air space per leaf area, S_{mes}/S was calculated from light and TEM micrographs as $\gamma \times L_{mes}/W$, where W is the width of the section measured, L_{mes} is the total length of mesophyll cells facing the intercellular air space, and γ is the curvature correction factor obtained as a weighted average for palisade and spongy mesophyll according to Evans *et al.* (1994). Leaf dry mass per unit area (M_A) was determined by drying leaves in the oven at 70°C for 72 h. Leaf thickness (t_{leaf}) was measured from the light microscopy images. Leaf density was calculated as M_A/t_{leaf}.

Carbohydrate and lipid peroxidation analyses: Carbohydrates were extracted from mature leaves and roots according to Lundell *et al.* (2008). After gas-exchange and Chl fluorescence measurements, samples were collected around noon and immediately frozen in liquid nitrogen. The soluble sugar and starch contents were determined spectrophotometrically using a *SpectraMax Paradigm Multi-Mode Detection Platform* (*Molecular Devices*, USA) at 620 nm by the anthrone method with

a commercial standard kit (*Solarbio Life Science*, Beijing, China). Standard curves were derived using δ-d-(+)-glucose in 80% ethanol. The level of general lipid peroxidation was measured using modified thiobarbituric acid–malondialdehyde (TBA–MDA) methods (Hodges *et al.* 1999). Leaves were powdered in liquid nitrogen and homogenized in 5% TCA. Reaction buffer of 0.65% (w/v) TBA containing 20% TCA and 0.01% (w/v) butylated hydroxytoluene was mixed with an equal volume of supernatant. Absorption was measured using a *SpectraMax Paradigm Multi-Mode Detection Platform* (*Molecular Devices*, USA) at 532, 600, and 440 nm. The concentration of malondialdehyde per fresh mass was calculated.

Chl and xanthophyll cycle pigment analysis: Leaf pigments were extracted from the same frozen samples as described above. Leaf samples were grounded into powder in liquid N_2 with 80% acetone (Tóth *et al.* 2002). The extracts were centrifuged and the supernatant was collected and stored at –20°C until analysis. Chl content was measured according to Wellburn and Lichtenthaler (1984). Carotenoid content was determined as described by Hughes *et al.* (2012). The supernatant was filtered through 0.45-micron nylon filters (*Millipore*) and then analyzed using an HPLC/DAD system (*Agilent 1260 II*) equipped with a UV/VIS detector (*Agilent*). HPLC was performed on a *Prontosil* C18 column (*Prontosil 120-5-C18-ace-EPS*, dp: 5 µm, 250 × 4.6 mm, *Bischoff*, Leonberg, Germany). The flow rate was 2 ml min^{-1}. The mobile phases were solvent A (76% acetonitrile:17% methanol: 7% 0.1 M TRIS, pH 8.0; v/v) and solvent B (80% methanol:20% hexane; v/v) with gradient elution. Zeaxanthin was used as a standard for the identification of peaks in the chromatogram. Total xanthophyll cycle pigments (VAZ) were calculated as the sum of violaxanthin (V), antheraxanthin (A), and zeaxanthin (Z). De-epoxidation state of the xanthophyll cycle (DEPS) was expressed as (0.5A + Z)/(V + A + Z). Each analysis was repeated three times.

Statistical analysis: All of the measurements were performed four times, and the means and calculated standard deviations (SD) are reported. Differences were evaluated by one-way analysis of variance (*ANOVA*) and *Student*'s *t*-test with *Microsoft Excel 2016* (*Microsoft Inc.*), and *P*-values are shown in the figures with different letters ($P \leq 0.05$). Graphs were plotted with *Adobe Illustrator* software (*Adobe Systems*, Mountain View, CA, USA).

Results

Anatomical changes of *Populus* leaves: To study the plasticity of *Populus* under different growth conditions, we investigated the morphological and anatomical characteristics of the fully expanded leaves from tissue-culture clones grown in the phytotron (YC), the glasshouse (YG and MG), and the field (MF), where Y and M, respectively, represent leaves which were 2 and 4 month old and C, G, and F respectively, represent plants grown in the phytotron, glasshouse, and field (Fig. 1*A*; Table 1S,

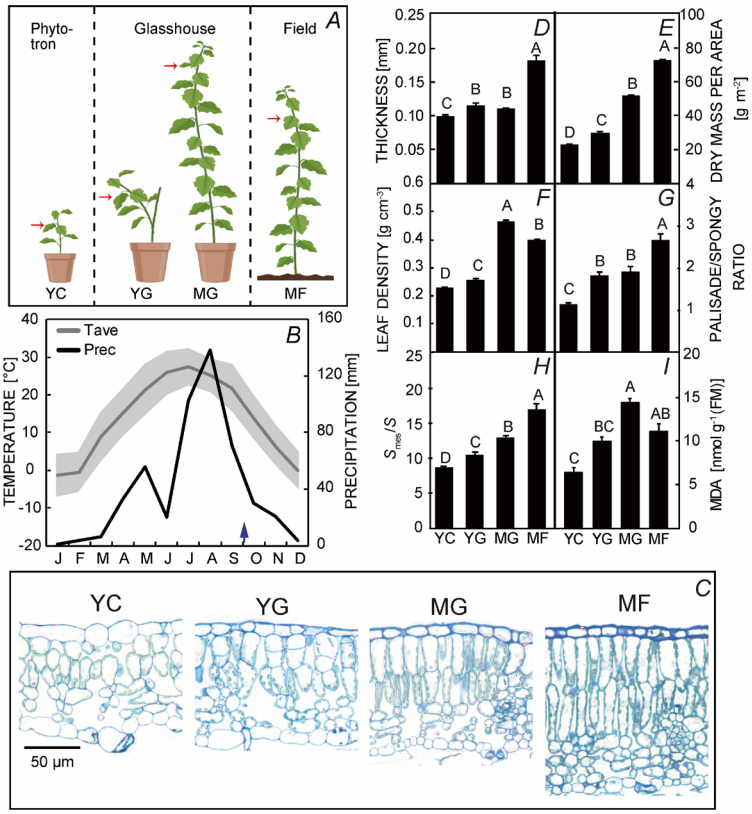

Fig. 1. The changes in the anatomy of *Populus alba* leaves. (*A*) The plants were grown under the phytotron (YC), the sunlit glasshouse (YG and MG), and the field (MF), respectively. The fully expanded leaves used for the experiment are indicated by *red arrows*. (*B*) The monthly average of temperature and precipitation data during 2019. (*C*) The light micrographs of leaf cross-sections, bar: 50 µm. Variations in leaf thickness (*D*), leaf dry mass per unit area (*E*), leaf density (*F*), the ratio of the palisade to spongy (*G*), mesophyll surface area exposed to intercellular air space per unit leaf area (*H*), and malondialdehyde (MDA) content (*I*). Significant differences are indicated with *different letters* above the bars (one-way *ANOVA*, $P<0.05$). Each data point represents the mean of four biological replicates.

supplement). All sampled leaves were fully developed under each growth condition.

The leaves from the field (MF) were thick, with thickened cell walls in the upper epidermal cells and high dry mass per area (DMA; Fig. 1*C*,*E*). The leaves from the phytotron (YC), grown under constant temperature and moderate light, were thin and their mean DMA was three times less than that of the field leaves. The morphological and anatomical characteristics of leaves from the glasshouse (MG and YG) fell in between the MF and YC leaves. The density of MG and MF leaves was 1.6–2.0 times higher than that of YC and YG leaves, suggesting the leaf density was more related to leaf age than growth conditions (Fig. 1*F*). These trends were similar for the palisade/spongy ratio, which in MF leaves was as high as 2.67 and in YC leaves was close to one (Fig. 1*G*). Mesophyll surface area exposed to the intercellular air spaces (S_{mes}/S) thus varied in leaves under different growth conditions (Fig. 1*H*). The elongated palisade cells in the leaves from the field increased exposure to the intercellular air spaces, while the roundish palisade cells in the YC leaves decreased exposure (Fig. 1*H*).

The chloroplast ultrastructure changes of *Populus* leaves: Analysis of the transmission electron micrographs (TEM) showed that the chloroplast ultrastructure underwent extensive remodeling of the thylakoid membranes under different growth conditions. The chloroplasts of the YC and YG leaves were full of thylakoid membranes (Fig. 2) and the grana diameter was significantly wider in the YC and YG leaves than that of the MG and MF leaves (Fig. 2). Large plastoglobules were commonly observed in the chloroplasts of MF leaves from the field but were rare in the chloroplasts of leaves from the phytotron and the glasshouse. There were also more and larger starch granules in the chloroplasts of both MG and MF leaves compared to the YC leaves from the phytotron (Fig. 2).

Nonstructural carbohydrate (NSC) accumulation: We tested the accumulated nonstructural carbohydrates (NSC) by separately examining soluble sugars and starch in leaves and roots. Soluble sugar mainly accumulated in the leaves, while starch mainly accumulated in the roots (Fig. 3). Higher NSC contents were measured in the MG and MF plantlets (Fig. 3). In line with the observations from the TEM images, both the MG and MF plantlets accumulated at least 2.7 times more starch in their leaves than YC and YG plantlets. Meanwhile, MG and MF plantlets transported starch to the roots 4.4 times more than the YC and YG plantlets (Fig. 3*B*). Although both YG and MG plantlets were grown in the glasshouse, two times more soluble sugar accumulated in MG leaves compared to YG leaves and 4.6 times more starch accumulated in the roots of MG than that of YG. The accumulation of NSC in YC plantlets was much lesser than that in other plants and mainly presented as soluble sugar in leaves (Fig. 3*A*). There was barely any starch accumulation in YC plantlets (Fig. 3*B*).

Leaf photosynthetic capacity: To investigate the physiological response of *Populus* towards different growth conditions, we analyzed the characteristics of CO_2 assimilation *via* gas exchange. The saturating CO_2 assimilation rate at 400 ppm CO_2 concentration (P_N) showed similar trends as the palisade/spongy ratio (Figs. 1, 4*A*). The P_N in the field leaves was four times as high as in phytotron leaves, and the leaf samples from the glasshouse showed medium CO_2 assimilation rates (Fig. 4*A*). Both stomatal conductance (g_s) and transpiration rate (E) showed no significant difference between leaves from the field and glasshouse but were 1.7–3.1 times higher than those of YC leaves (Fig. 4*C*,*E*). It is worth noting that mesophyll conductance (g_m) was the highest in the MF leaves, which correlates with S_{mes}/S and P_N (Figs. 1*F*, 4*D*). These results suggest changes in within-leaf diffusion and may contribute to constrained photosynthetic capacity in *Populus*.

To study the limitation of P_N, we analyzed the response of P_N to varying leaf internal CO_2 concentrations (C_i; Fig. 4*A*). The photosynthetic capacity shown by the P_N/C_i curve was consistent with the changes of P_N (Fig. 5*A*). The MF leaves had a higher CO_2 assimilation capacity than

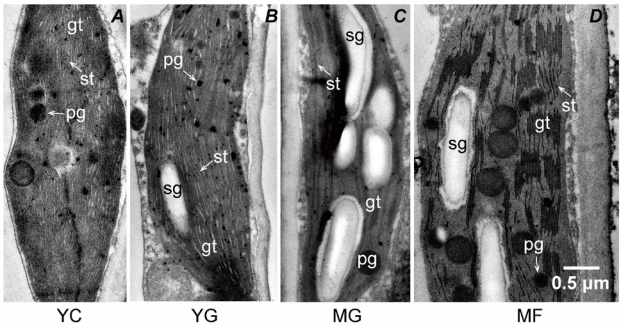

Fig. 2. Transmission electron micrographs (TEM) of chloroplast structures in *Populus alba* leaves under different growth conditions. Representative images are shown. Bar: 0.5 µm. gt – grana thylakoid (stacked), st – stromal thylakoid (unstacked), pg – plastoglobulus.

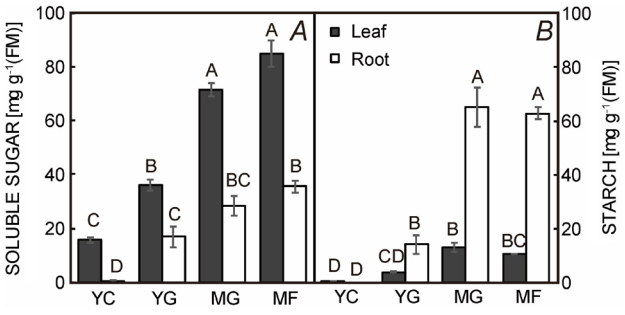

Fig. 3. The soluble sugar (*A*) and starch (*B*) contents in *Populus alba* under different growth conditions. Soluble sugars and starch per fresh matter in leaves (*black bars*) and roots (*white bars*). Each bar is the average obtained from samples of $n = 4$ (± SE). Significant differences are indicated with *different letters* above the bars (one-way *ANOVA*, $P<0.05$).

leaves grown in the glasshouse, and the YC leaves had the lowest assimilation capacity (Fig. 4*A*). Coordinately, the MF leaves showed the highest maximum carboxylation rate of Rubisco (V_{cmax}) and the regeneration rate of ribulose 1,5-bisphosphate (RuBP, J_{max}). The V_{cmax} of MF was 10 times higher than that of YC (Fig. 5*B*). Analysis of the balance between RuBP regeneration and carboxylation showed the J_{max}/V_{cmax} ratio of 2.38 in the YC leaves, while that in the MF leaves was close to 1 (Fig. 5*D*). The lower ratio observed in the field leaves may be partly explained by the greater plasticity of V_{cmax} towards growth condition variations.

The limiting step of P_N was analyzed based on the limitation by either RuBP carboxylation (A_c) or RuBP regeneration (A_j). The Rubisco carboxylation limitation on P_N was most significant in MF leaves where small changes in C_i resulted in substantial changes in P_N (Fig. 1S, *supplement*). Coordinately, the stomatal limitation was the greatest in leaves from the field than that from the glasshouse or phytotron (Fig. 5*E*). P_N was mainly limited by A_c at low C_i and by A_j at high C_i, except the P_N of YC leaves was limited by A_j irrespective of C_i (Fig. 1S). Those results suggest that in the *Populus* leaves with high J_{max}/V_{cmax} ratios, the limitation of P_N by RuBP regeneration was aggravated, especially in leaves from the phytotron (Figs. 5*D*, 1S).

Photosynthetic performances of PSI and PSII: Measurements of Chl fluorescence demonstrated the photosynthetic performance of all *Populus* plants maintained a fully functional photosynthetic electron transport chain, with a maximum PSII quantum yield (F_v/F_m) of around 0.8 (Fig. 2S, *supplement*). Consistent with the photosynthetic capacity as shown by the P_N/C_i curve, the electron transport rates of both PSII [$ETR_{(II)}$] and PSI [$ETR_{(I)}$] were the highest in the MF leaves (Fig. 6*A*,*B*). The $ETR_{(II)}$ in the YC leaves decreased when light intensity increased,

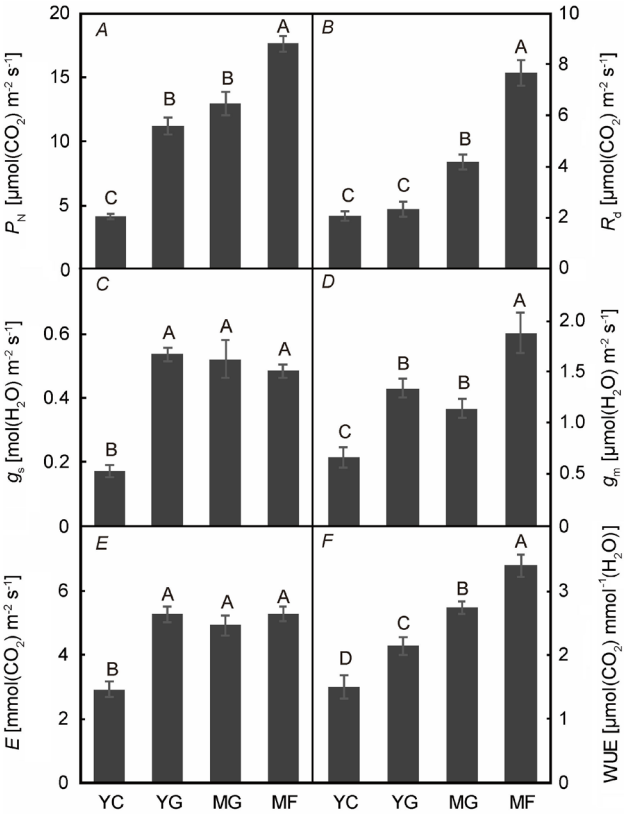

Fig. 4. The gas-exchange parameters in *Populus alba* under different growth conditions. (*A*) The net assimilation rate (P_N), (*B*) the respiration rate under light (R_d), (*C*) stomatal conductance (g_s), (*D*) mesophyll conductance (g_m), (*E*) transpiration rate (E), and (*F*) intrinsic water-use efficiency (WUE) of *Populus alba* leaves under different growth conditions. Each bar is the average obtained from samples of $n = 4$ (± SE). *Different letters* above bars denote statistically significant differences between treatments at the $P<0.05$ according to one-way *ANOVA*.

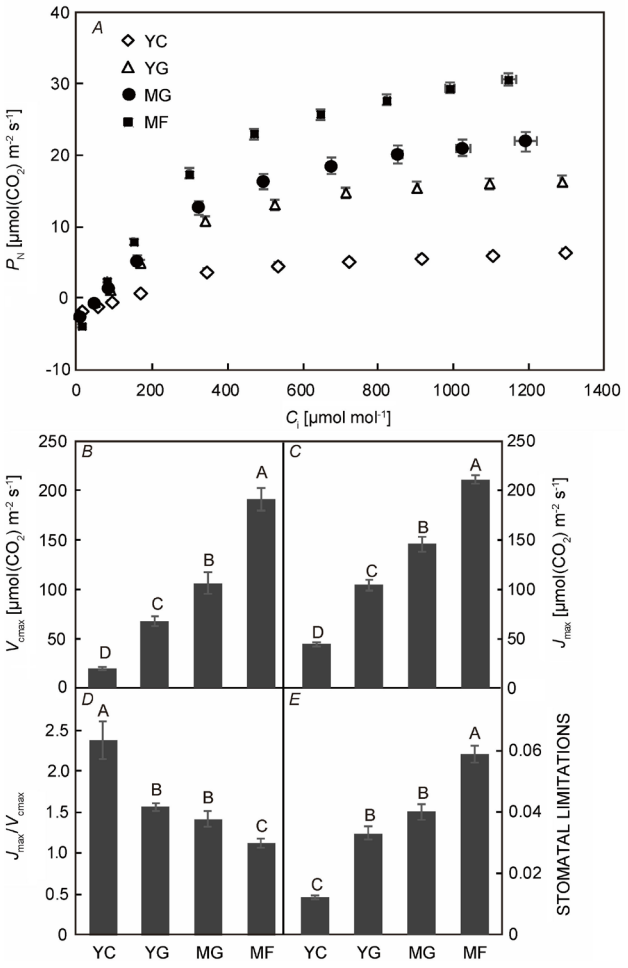

Fig. 5. The capacity for CO_2 assimilation in *Populus alba* under different growth conditions. (*A*) Response of assimilation (P_N) to the internal CO_2 concentration (C_i) and (*B*) maximum rate of carboxylation (V_{cmax}), (*C*) maximum rate of electron transport (J_{max}), (*D*) the ratio of J_{max} to V_{cmax}, and (*E*) stomatal limitation. Each bar is the average obtained from samples of $n = 4$ (± SE). *Different letters* above bars denote statistically significant differences between treatments at the $P<0.05$ according to one-way *ANOVA*.

suggesting significant photoinhibition under high light (Fig. 6*A*). The ratio of $ETR_{(I)}$ to $ETR_{(II)}$ was close to 1 at low light and subsequently increased with the increase in light intensity in all leaves. However, the $ETR_{(I)}/ETR_{(II)}$ ratio of YC leaves increased more than 3 times as light intensity increased, unlike in the MG and MF leaves (Fig. 6*C*), mainly due to decreased $ETR_{(II)}$ (Fig. 7).

Protective mechanisms *via* NPQ dissipate excess excitation energy as heat. The NPQ of poplars from the field and glasshouse were more than 1.9 times higher than those from the phytotron (Fig. 6*D*). The NPQ of the leaves from the field and glasshouse increased from approximately 0.7 to 1.9 under high light and then recovered to 0.5 in the dark (Fig. 6*D*), while the NPQ of the phytotron

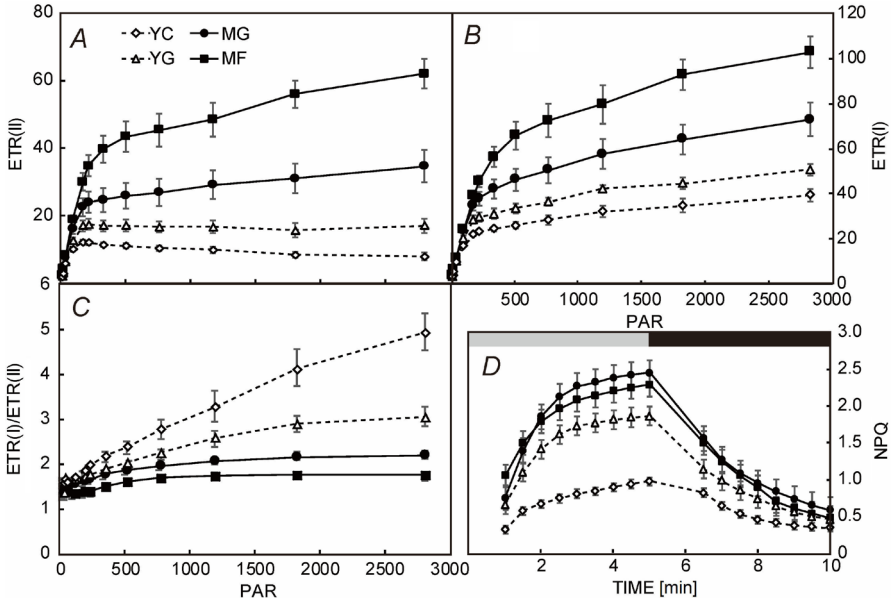

Fig. 6. The electron transport parameters of the light curve and the nonphotochemical quenching (NPQ) of *Populus alba*. (*A*) Electron transport rate through PSII [$ETR_{(II)}$], (*B*) electron transport rate through PSI [$ETR_{(I)}$], (*C*) the ratio of $ETR_{(I)}$ to $ETR_{(II)}$, and (*D*) nonphotochemical quenching (NPQ) in analyzed leaf samples. The photosynthetic fluorescence was measured under high light (indicated in *gray*, *top bar*) and then under dark (*black*). Points represent mean (± SE) from samples of $n = 4$.

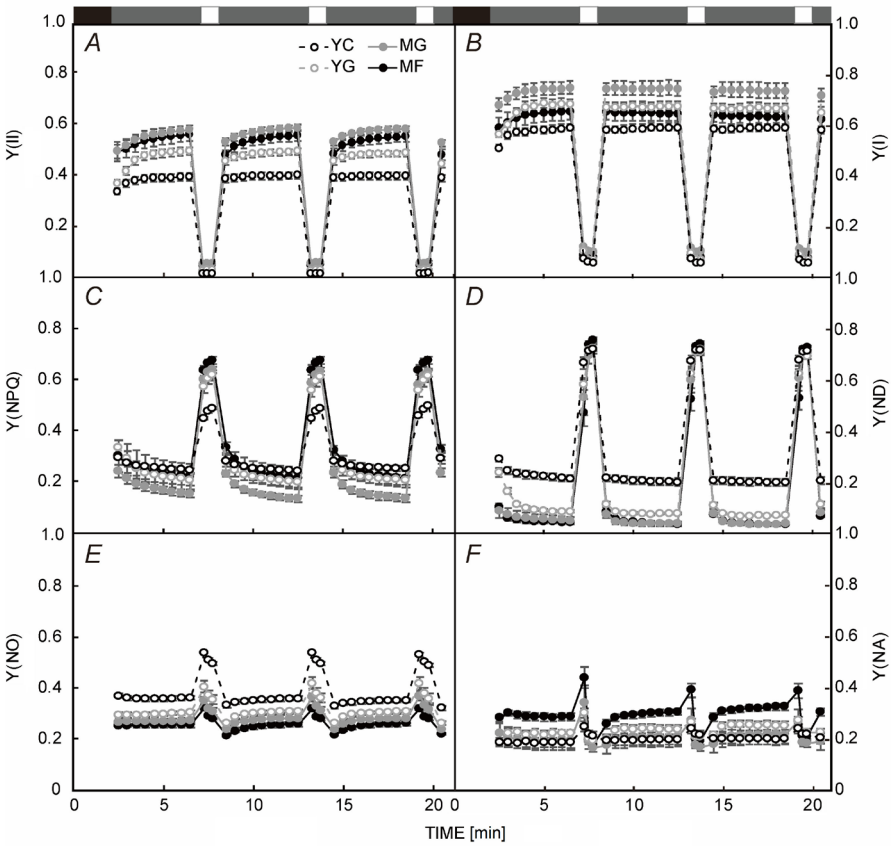

Fig. 7. Photosynthetic parameters upon light fluctuations in *Populus alba* under different growth conditions. (*A*) Operating efficiency of PSII [$Y_{(II)}$], (*B*) operating efficiency of PSI [$Y_{(I)}$], (*C*) quantum yield of regulated energy dissipation of PSII [$Y_{(NPQ)}$], (*D*) quantum yield of nonphotochemical energy dissipation in PSI reaction centers that are limited due to a shortage of electrons (donor-side limitation) [$Y_{(ND)}$], (*E*) quantum yield of nonregulated energy dissipation of PSII [$Y_{(NO)}$], (*F*) quantum yield of nonphotochemical energy dissipation in PSI reaction centers that are limited due to shortage of electron acceptors (acceptor-side limitation) [$Y_{(NA)}$]. Photosynthetic fluorescence was measured under 2-min dark (indicated in *black*, *top bar*) and then under low light [59 μmol(photon) m^{-2} s^{-1}; *gray*] which was interrupted by 1 min of high light [1,455 μmol(photon) m^{-2} s^{-1}; *white*] every 5 min on leaves (biological replicates $n = 4$, mean ± SE).

leaves changed within a narrow range between 0.3 to 1.0 (Fig. 6*D*).

The regulatory mechanisms of photosynthetic light reactions: Apart from NPQ protection, cyclic electron transport (CET) could constitute a safety valve for the avoidance of over-reduction of PSI under an abrupt increase in light, protecting the photosystems from deleterious effects of excess excitation energy. We performed a fluctuating light experiment including periods of high light to monitor the photochemical efficiency of PSI and PSII simultaneously. $Y_{(II)}$ and $Y_{(I)}$ did not decrease after several high-light periods, suggesting the photosynthetic machinery of all poplar samples was protected from fluctuating light (Fig. 7*A*,*B*). For the leaves from the field and glasshouse, the increase of $Y_{(NPQ)}$ when shifting from low light to high light exceeded the increase in the leaves from the phytotron by a factor of 2. In contrast, the YC leaves showed higher values of $Y_{(NO)}$ than that of leaves from the field and glasshouse. High $Y_{(NO)}$ values indicated the excess light energy was not dissipated by regulation, suggesting an overaccumulation of ROS. For PSI, $Y_{(ND)}$ indicates a donor-side limitation, which explains the levels of oxidized P_{700}. The $Y_{(ND)}$ in the YC leaves under low light was the highest, but was as high as in the YG, MG, and MF leaves under high light (Fig. 7*D*). $Y_{(NA)}$ indicates an acceptor side limitation of PSI. The $Y_{(NA)}$ in the field leaves was transiently induced when shifting to high light and then decreased with a corresponding increase in $Y_{(ND)}$ (Fig. 7*F*). This transient induction of $Y_{(NA)}$ was less pronounced in the YC, YG, and MG leaves.

Content of chlorophylls and xanthophyll cycle components: The leaves from *Populus* grown in the field contained 50% less Chl *a* and *b* and 65% less lutein compared to *Populus* grown in the phytotron and glasshouse (Fig. 8). However, the Chl *a*/*b* ratio was higher in the field leaves than that in the leaves from the phytotron or glasshouse (Fig. 8*C*). The amount of xanthophyll cycle pigments (VAZ) did not significantly differ between all samples (Fig. 8*E*). The MG and MF leaves showed higher de-epoxidation states of the xanthophyll cycle (DEPS) than that of the YC and YG leaves (Fig. 8*F*). DEPS was around 0.4 in the MG and MF leaves, which was three times higher than that in the YC and YG leaves (Fig. 8*F*).

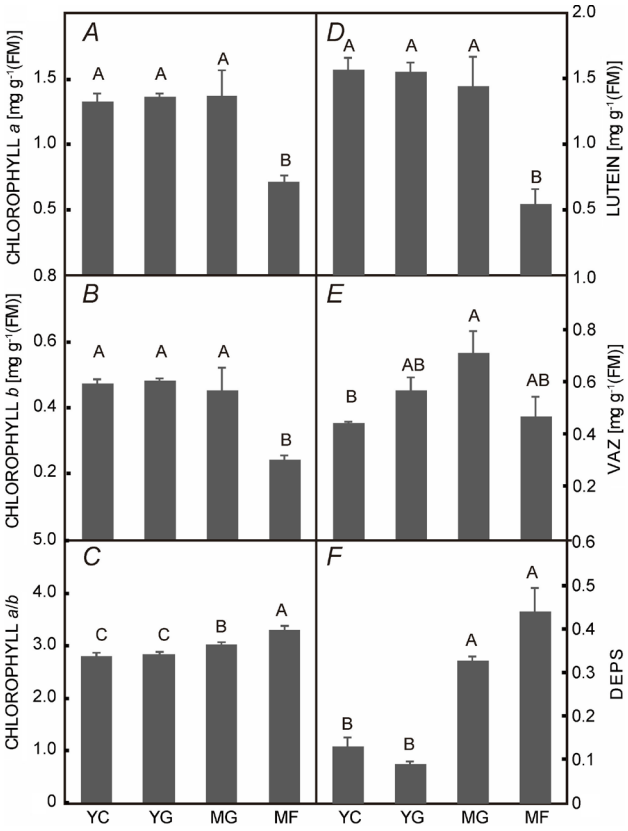

Fig. 8. Changes in leaf pigments of *Populus alba* under different growth conditions. (*A*) and (*B*), chlorophyll *a* and *b* expressed per gram fresh mass, (*C*) Chl *a*/*b*, the ratio of chlorophyll *a* to chlorophyll *b*, (*D*) the content of lutein per gram fresh mass, (*E*) VAZ, total xanthophyll cycle pool, comprised of violaxanthin, antheraxanthin, and zeaxanthin, (*F*) DEPS, the de-epoxidation of the xanthophyll cycle. Bars represent mean (± SE) from samples of $n = 3$. *Different letters* above bars denote statistically significant differences between treatments at the $P<0.05$ according to one-way *ANOVA*.

Discussion

Understanding the regulatory mechanisms of trees to environmental changes is one of the key goals for forest genetics and tree breeding, however, most studies to date were performed under controlled laboratory conditions to study the response to specific environmental factors. In the field, light, temperature, water availability, and other environmental factors are constantly fluctuating in the transient, diurnal, and seasonal patterns, which greatly increases the difficulty of understanding tree responses in natural forests (Morales and Kaiser 2020).

Here, we investigated the morphological and physiological responses of fully expanded poplar leaves that emerged under three growth conditions, using trees from the same clone to minimize the effect of genetic variation. The three growth conditions were under a phytotron with constant light and temperature, in a glasshouse with fluctuating semi-natural conditions, and in the field. To control environment variables as much as possible to increase comparability, all plants were irrigated and fertilized regularly. Moreover, all indoor poplars were grown under long-day conditions approximating the natural photoperiod of the season, and the temperature in the phytotron (25°C) was around the mean of the field temperatures that ranged between 20 and 30°C (Fig. 1*B*). The major differences between the three growth conditions were light intensity and the variability of light and temperature. The fluctuations of temperature and light intensity were the highest in the field, the lowest in the phytotron, and the middle for the glasshouse. In addition, root restriction is one of the factors in photosynthetic acclimation (Thomas and Strain 1991). The growth of the

roots did not only affect the water and nutrition utilization but also affect the source–sink balance, which was a possible mechanism for regulating net photosynthesis. Since the roots of field-grown *P. alba* were not restricted by pots, the root growth may also play a role in influencing photosynthetic efficiency.

Our results indicated that P_N and anatomical characteristics, such as leaf thickness and palisade/spongy ratio, significantly differed under the three growth conditions (Fig. 1). The leaves from the field showed the highest P_N and mesophyll conductance (g_m), whereas their stomatal conductance (g_s) was similar to the leaves from the glasshouse (Fig. 3). Mesophyll conductance from intercellular cavities to chloroplasts significantly constrains P_N (Flexas *et al.* 2008). The high palisade/spongy ratio and S_{mes}/S in the field leaves contributed to increased exposure to the intercellular air spaces, which increased CO_2 supply for carbon fixation. The development of leaves was also altered by the growth conditions (Schumann *et al.* 2017, Brestic *et al.* 2018, Morales and Kaiser 2020). The internal architecture development of poplar leaves was delayed under the phytotron condition (YC *vs*. YG) and the glasshouse condition (MG *vs*. MF) as shown in Fig. 1*C*. Consequently, g_m may be the key limiting factor of photosynthesis at the leaf developing stage (Tosens *et al.* 2012). Daily fluctuating temperature and high light have direct effects on enzyme activities and diffusion-dependent processes (Schumann *et al.* 2017, Brestic *et al.* 2018), which may then induce major changes in leaf anatomy, P_N, and g_m.

Fluctuations in light induce photodamage if the plants do not possess efficient protective mechanisms (Allahverdiyeva *et al.* 2015, Fristedt *et al.* 2017, Kono *et al.* 2017). Once photodamage occurs, swelling of the thylakoid lumen or a bulging of the periphery of the thylakoid grana is often observed, and eventually the total thylakoid membrane and grana number in chloroplasts decreases (Kirchhoff 2019). The thylakoids in the chloroplasts appeared to be undamaged and the malondialdehyde (MDA) content was similar in samples from the glasshouse and the field (Figs. 1*I*, 2). In addition, the F_v/F_m was about 0.8 and showed no significant difference between all poplar samples (Fig. 2S). These results suggested that PSII photochemistry was hardly affected under fluctuating conditions. Plastoglobules are composed of lipoproteins and small antioxidant molecules such as tocopherols (Vidi *et al.* 2006, Bréhélin *et al.* 2007). The antioxidant tocopherols stored in plastoglobules protect membrane lipids from photooxidation and scavenge ROS (Havaux *et al.* 2005, Pérez-Llorca *et al.* 2019). In accordance, large plastoglobules were commonly observed in the chloroplasts of MF leaves from the field but were rare in the chloroplasts of leaves from the phytotron and the glasshouse (Fig. 2). It is tempting to speculate that the enlargement of plastoglobules with abundant tocopherols contributed to the photoprotection of poplar.

In addition to the anatomical and ultrastructural plasticity, the poplar has highly effective photosynthesis regulatory mechanisms for photoprotection under natural growth conditions. For PSII, zeaxanthin- and ΔpH-dependent NPQ of excess excitation energy is considered to be one of the major PSII photoprotective mechanisms (Kreslavski *et al.* 2017, Velitchkova *et al.* 2020). The range of NPQ regulation was wider in the field leaves than the phytotron leaves suggesting the well-developed NPQ capacity plays a role in photoprotection for plants grown under fluctuating conditions (Fig. 6). The capacity of thermal dissipation of absorbed energy was also shown by the de-epoxidation state of the xanthophyll cycle which was higher in the field samples (Fig. 8).

PGR5-dependent cyclic electron transport forms a large electron sink when the stroma is highly reduced and protects both photosystems from photodamage in fluctuating light (Yamamoto and Shikanai 2019). We performed a fluctuating light experiment to monitor the photochemical efficiency of PSI and PSII simultaneously (Fig. 7). A previous study of a similar fluctuating light experiment showed that PSII and PSI yield progressively decreased after several high-light periods in the wild type of *Arabidopsis* and rice, and an abrupt decline was present in *pgr5* mutant (Yamamoto *et al.* 2016, Nikkanen *et al.* 2018, Wada *et al.* 2018). However, the results in this study showed that $Y_{(II)}$ and $Y_{(I)}$ did not decrease after several high-light periods in all poplar samples (Fig. 7). In addition, both Scots pine and Norway spruce showed a steady or even increase in PSII and PSI yield after high-light periods (Yang *et al.* 2020). $Y_{(NA)}$ represents the acceptor-side limitation of PSI which contributes to photoinhibition of PSI. The significant reduction of $Y_{(NA)}$ to minimal levels during high-light periods presented in the MF leaves (Fig. 7*F*) indicates that the PSI was well protected against photoinhibition (Huang *et al.* 2010, Yang *et al.* 2020, Zhao *et al.* 2021). It is reasonable to assume that the photosynthetic machinery was well protected from fluctuating light in trees such as poplar and conifers, although details of photoprotection during fluctuating light and underlying molecular mechanisms require further investigation.

In conclusion, the leaves of *Populus* seem to have recruited a suit of strategies that fine-tunes their anatomical characteristics and their whole photosynthetic machinery in response to naturally fluctuating conditions. The plasticity of structure and physiology in the face of a fluctuating environment may play a key role in the strong environmental adaptability of poplar. Future studies on the effects of stress using young seedlings grown under constant conditions should take into consideration this acclimation flexibility.

References

Ahmad P., Jaleel C.A., Salem M.A. *et al.*: Roles of enzymatic and nonenzymatic antioxidants in plants during abiotic stress. – Crit. Rev. Biotechnol. **30**: 161-175, 2010.

Ahmad P., Tripathi D.K., Deshmukh R. *et al.*: Revisiting the role of ROS and RNS in plants under changing environment. – Environ. Exp. Bot. **161**: 1-3, 2019.

Allahverdiyeva Y., Suorsa M., Tikkanen M., Aro E.-M.: Photoprotection of photosystems in fluctuating light

intensities. – J. Exp. Bot. **66**: 2427-2436, 2015.
Allakhverdiev S.I.: Optimising photosynthesis for environmental fitness. – Funct. Plant Biol. **47**: iii-vii, 2020.
Baker N.R.: Chlorophyll fluorescence: a probe of photosynthesis in vivo. – Annu. Rev. Plant Biol. **59**: 89-113, 2008.
Bigras F.J., Bertrand A.: Responses of *Picea mariana* to elevated CO_2 concentration during growth, cold hardening and dehardening: phenology, cold tolerance, photosynthesis and growth. – Tree Physiol. **26**: 875-888, 2006.
Bréhélin C., Kessler F., van Wijk K.J.: Plastoglobules: versatile lipoprotein particles in plastids. – Trends Plant Sci. **12**: 260-266, 2007.
Brestic M., Yang X., Li X., Allakhverdiev S.I.: Crop photosynthesis for the twenty-first century. – Photosynth. Res. **150**: 1-3, 2021.
Brestic M., Zivcak M., Hauptvogel P. *et al.*: Wheat plant selection for high yields entailed improvement of leaf anatomical and biochemical traits including tolerance to non-optimal temperature conditions. – Photosynth. Res. **136**: 245-255, 2018.
Brundu G., Lupi R., Zapelli I. *et al.*: The origin of clonal diversity and structure of *Populus alba* in Sardinia: Evidence from nuclear and plastid microsatellite markers. – Ann. Bot.-London **102**: 997-1006, 2008.
Demmig-Adams B., Adams III W.W.: An integrative approach to photoinhibition and photoprotection of photosynthesis. – Environ. Exp. Bot. **154**: 1-3, 2018.
Demmig-Adams B., Cohu C.M., Muller O., Adams III W.W.: Modulation of photosynthetic energy conversion efficiency in nature: from seconds to seasons. – Photosynth. Res. **113**: 75-88, 2012.
Demmig-Adams B., Muller O., Stewart J.J. *et al.*: Chloroplast thylakoid structure in evergreen leaves employing strong thermal energy dissipation. – J. Photoch. Photobio. B **152**: 357-366, 2015.
Dlugos D.M., Collins H., Bartelme E.M., Drenovsky R.E.: The non-native plant *Rosa multiflora* expresses shade avoidance traits under low light availability. – Am. J. Bot. **102**: 1323-1331, 2015.
Ensminger I., Schmidt L., Lloyd J.: Soil temperature and intermittent frost modulate the rate of recovery of photosynthesis in Scots pine under simulated spring conditions. – New Phytol. **177**: 428-442, 2008.
Evans J.R., von Caemmerer S., Setchell B.A., Hudson G.S.: The relationship between CO_2 transfer conductance and leaf anatomy in transgenic tobacco with a reduced content of Rubisco. – Funct. Plant Biol. **21**: 475-495, 1994.
Farquhar G.D., von Caemmerer S., Berry J.A.: A biochemical model of photosynthetic CO_2 assimilation in leaves of C_3 species. – Planta **149**: 78-90, 1980.
Flexas J., Ribas-Carbó M., Diaz-Espejo A. *et al.*: Mesophyll conductance to CO_2: current knowledge and future prospects. – Plant Cell Environ. **31**: 602-621, 2008.
Fristedt R., Trotta A., Suorsa M. *et al.*: PSB33 sustains photosystem II D1 protein under fluctuating light conditions. – J. Exp. Bot. **68**: 4281-4293, 2017.
Havaux M., Eymery F., Porfirova S. *et al.*: Vitamin E protects against photoinhibition and photooxidative stress in *Arabidopsis thaliana*. – Plant Cell **17**: 3451-3469, 2005.
Hodges D.M., DeLong J.M., Forney C.F., Prange R.K.: Improving the thiobarbituric acid-reactive-substances assay for estimating lipid peroxidation in plant tissues containing anthocyanin and other interfering compounds. – Planta **207**: 604-611, 1999.
Hozain M.I., Salvucci M.E., Fokar M., Holaday S.A.: The differential response of photosynthesis to high temperature for a boreal and temperate *Populus* species relates to differences in Rubisco activation and Rubisco activase properties. – Tree Physiol. **30**: 32-44, 2010.
Huang W., Hu H., Zhang S.B.: Photosynthetic regulation under fluctuating light at chilling temperature in evergreen and deciduous tree species. – J. Photoch. Photobio. B **219**: 112203, 2021.
Huang W., Zhang S.B., Cao K.F.: Stimulation of cyclic electron flow during recovery after chilling-induced photoinhibition of PSII. – Plant Cell Physiol. **51**: 1922-1928, 2010.
Hughes N.M., Burkey K.O., Cavender-Bares J., Smith W.K.: Xanthophyll cycle pigment and antioxidant profiles of winter – red (anthocyanic) and winter – green (acyanic) angiosperm evergreen species. – J. Exp. Bot. **63**: 1895-1905, 2012.
IPCC: Climate Change 2014: Synthesis Report. Contribution of Working Groups I, II and III to the Fifth Assessment Report of the Intergovernmental Panel on Climate Change. Pp. 151. IPCC, Geneva 2014.
Kirchhoff H.: Structural changes of the thylakoid membrane network induced by high light stress in plant chloroplasts. – Philos. T. Roy. Soc. B **369**: 20130225, 2014.
Kirchhoff H.: Chloroplast ultrastructure in plants. – New Phytol. **223**: 565-574, 2019.
Kohli S.K., Khanna K., Bhardwaj R. *et al.*: Assessment of subcellular ROS and NO metabolism in higher plants: multifunctional signaling molecules. – Antioxidants **8**: 641, 2019.
Kono M., Yamori W., Suzuki Y., Terashima I.: Photoprotection of PSI by far-red light against the fluctuating light-induced photoinhibition in *Arabidopsis thaliana* and field-grown plants. – Plant Cell Physiol. **58**: 35-45, 2017.
Korotaeva N., Romanenko A., Suvorova G. *et al.*: Seasonal changes in the content of dehydrins in mesophyll cells of common pine needles. – Photosynth. Res. **124**: 159-169, 2015.
Kreslavski V.D., Brestic M., Zharmukhamedov S.K. *et al.*: Mechanisms of inhibitory effects of polycyclic aromatic hydrocarbons in photosynthetic primary processes in pea leaves and thylakoid preparations. – Plant Biol. **19**: 683-688, 2017.
Li L., Aro E.-M., Millar A.H.: Mechanisms of photodamage and protein turnover in photoinhibition. – Trends Plant Sci. **23**: 667-676, 2018.
Li Z., Wakao S., Fischer B.B., Niyogi K.K.: Sensing and responding to excess light. – Annu. Rev. Plant Biol. **60**: 239-260, 2009.
Liu Y.-J., Wang X.-R., Zeng Q.-Y.: De novo assembly of white poplar genome and genetic diversity of white poplar population in Irtysh River basin in China. – Sci. China Life Sci. **62**: 609-618, 2019.
Lundell R., Saarinen T., Åström H., Hänninen H.: The boreal dwarf shrub*Vaccinium vitis-idaea* retains its capacity for photosynthesis through the winter. – Botany **86**: 491-500, 2008.
Morales A., Kaiser E.: Photosynthetic acclimation to fluctuating irradiance in plants. – Front. Plant Sci. **11**: 268, 2020.
Müller A., Leuschner C., Horna V., Zhang C.: Photosynthetic characteristics and growth performance of closely related aspen taxa: On the systematic relatedness of the Eurasian *Populus tremula* and the North American *P. tremuloides*. – Flora **207**: 87-95, 2012.
Nikkanen L., Toivola J., Trotta A. *et al.*: Regulation of cyclic electron flow by chloroplast NADPH-dependent thioredoxin system. – Plant Direct **2**: e00093, 2018.
Pérez-Llorca M., Casadesús A., Müller M., Munné-Bosch S.: Leaf orientation as part of the leaf developmental program

in the semi-deciduous shrub, *Cistus albidus* L.: Diurnal, positional, and photoprotective effects during winter. – Front. Plant Sci. **10**: 767, 2019.
Pfündel E., Klughammer C., Schreiber U.: Monitoring the effects of reduced PS II antenna size on quantum yields of photosystems I and II using the Dual-PAM-100 measuring system. – PAM Application Notes **1**: 21-24, 2008.
Saxe H., Cannell M.G.R., Johnsen Ø. *et al.*: Tree and forest functioning in response to global warming. – New Phytol. **149**: 369-399, 2002.
Schumann T., Paul S., Melzer M. *et al.*: Plant growth under natural light conditions provides highly flexible short-term acclimation properties toward high light stress. – Front. Plant Sci. **8**: 681, 2017.
Sharkey T.D., Bernacchi C.J., Farquhar G.D., Singsaas E.L.: Fitting photosynthetic carbon dioxide response curves for C_3 leaves. – Plant Cell Environ. **30**: 1035-1040, 2007.
Shikanai T., Yamamoto H.: Contribution of cyclic and pseudo-cyclic electron transport to the formation of proton motive force in chloroplasts. – Mol. Plant **10**: 20-29, 2017.
Stefanski A., Bermudez R., Sendall K.M. *et al.*: Surprising lack of sensitivity of biochemical limitation of photosynthesis of nine tree species to open-air experimental warming and reduced rainfall in a southern boreal forest. – Glob. Change Biol. **26**: 746-759, 2020.
Thomas R.B., Strain B.R.: Root restriction as a factor in photosynthetic acclimation of cotton seedlings grown in elevated carbon dioxide. – Plant Physiol. **96**: 627-634, 1991.
Tosens T., Niinemets Ü., Vislap V. *et al.*: Developmental changes in mesophyll diffusion conductance and photosynthetic capacity under different light and water availabilities in *Populus tremula*: how structure constrains function. – Plant Cell Environ. **35**: 839-856, 2012.
Tóth V.R., Mészáros I., Veres S., Nagy J.: Effects of the available nitrogen on the photosynthetic activity and xanthophyll cycle pool of maize in field. – J. Plant Physiol. **159**: 627-634, 2002.
Velitchkova M., Popova A.V., Faik A. *et al.*: Low temperature and high light dependent dynamic photoprotective strategies in *Arabidopsis thaliana*. – Physiol. Plantarum **170**: 93-108, 2020.
Vidi P.-A., Kanwischer M., Baginsky S. *et al.*: Tocopherol cyclase (VTE1) localization and vitamin E accumulation in chloroplast plastoglobule lipoprotein particles. – J. Biol. Chem. **281**: 11225-11234, 2006.
Wada S., Yamamoto H., Suzuki Y. *et al.*: Flavodiiron protein substitutes for cyclic electron flow without competing CO_2 assimilation in rice. – Plant Physiol. **176**: 1509-1518, 2018.
Ware M.A., Giovagnetti V., Belgio E., Ruban A.V.: PsbS protein modulates non-photochemical chlorophyll fluorescence quenching in membranes depleted of photosystems. – J. Photoch. Photobio. B **152**: 301-307, 2015.
Way D.A., Pearcy R.W.: Sunflecks in trees and forests: from photosynthetic physiology to global change biology. – Tree Physiol. **32**: 1066-1081, 2012.
Wellburn A.R., Lichtenthaler H.: Formulae and program to determine total carotenoids and chlorophylls *a* and *b* of leaf extracts in different solvents. – In: Sybesma C. (ed.): Advances in Photosynthesis Research. Advances in Agricultural Biotechnology. Vol. 2. Pp. 9-12. Springer, Dordrecht 1984.
Yamamoto H., Shikanai T.: PGR5-dependent cyclic electron flow protects photosystem I under fluctuating light at donor and acceptor sides. – Plant Physiol. **179**: 588-600, 2019.
Yamamoto H., Takahashi S., Badger M.R., Shikanai T.: Artificial remodelling of alternative electron flow by flavodiiron proteins in *Arabidopsis*. – Nat. Plants **2**: 16012, 2016.
Yang Q., Blanco N.E., Hermida-Carrera C. *et al.*: Two dominant boreal conifers use contrasting mechanisms to reactivate photosynthesis in the spring. – Nat. Commun. **11**: 128, 2020.
Zadworny M., Comas L.H., Eissenstat D.M.: Linking fine root morphology, hydraulic functioning and shade tolerance of trees. – Ann. Bot.-London **122**: 239-250, 2018.
Zhang S., Jiang H., Peng S. *et al.*: Sex-related differences in morphological, physiological, and ultrastructural responses of *Populus cathayana* to chilling. – J. Exp. Bot. **62**: 675-686, 2011.
Zhao W., Zhang Q.S., Tan Y. *et al.*: Photoprotective roles of ascorbate and PSII cyclic electron flow in the response of the seagrass *Zostera marina* to oxygen-evolving complex photoinactivation. – Photosynthetica **59**: 600-605, 2021.